DESIGN PROCEDURES FOR IMPROVED LAMINATE PERFORMANCE IN BENDING AND EXTENSION

H. S. J. Lee[1] and C. B. York[2]

[1] University of Glasgow, United Kingdom, h.lee.2@research.gla.ac.uk, https://www.gla.ac.uk/schools/engineering/staff/jasonlee/

[2] Singapore Institute of Technology, Singapore, Christopher.York@singaporetech.edu.sg, https://www.singaporetech.edu.sg/directory/faculty/christopher-bronn-york

Keywords: Bending-Twisting Coupling, Extension-Shearing Coupling, Double angle-ply laminates, Standard ply laminates, Buckling

ABSTRACT

This article discusses improved laminate performance relating to both in-plane properties (e.g. first ply failure) and out-of-plane properties (e.g. initial buckling) using double angle-ply laminates (with $\pm\psi$ and $\pm\phi$ ply orientations), which are stiffness matched to standard laminate configurations.
A procedure for producing isotropic laminates in bending, is first employed. Off-axis orientation is then applied to these designs to maximise *Extension-Shearing* coupling; bending isotropy is unaffected by off-axis alignment, hence buckling performance is also unchanged. The performance of competing *Extension-Shearing* coupled designs are then assessed against a first ply failure strength criterion.

1 INTRODUCTION

Aero-elastic tailoring of composite wings is expected to lead to a valuable drag reduction mechanism in conventional swept back wings [1], by reducing any fluctuation away from the optimized static cruise configuration, i.e., reducing the magnitude of wing twists as it bends. Drag reduction can be achieved by introducing passive bending-twisting coupling behaviour (a so-called passive-adaptive wing), to maintain a constant angle of attack across the wing, irrespective of the magnitude of the bending deflections [2]. This has been demonstrated for a number of competing laminate tailoring techniques, generally requiring off-axis material alignment to achieve *Extension-Shearing* coupled properties. The focus of the previous work has so far been restricted to stiffness tailoring, hence the effect of such tailoring on the laminate performance is now considered. This is assessed by a combination of initial buckling within material strength constraints.

Studies on buckling optimization of composite laminates under strength constraints are summarised elsewhere [3], whereby strength constraints are applied through a maximum laminate strain, or by assessing individual ply stresses [4]. This includes methods for optimal stacking sequences to maximising buckling [5] and the use of different failure criteria [6].

No studies have previously been conducted on the assessment of buckling under material strength constraints for off-axis aligned materials with *Extension-Shearing* coupling behaviour. The objective of this study is therefore to access the available design spaces for a number of design solutions, including double angle-ply laminates and standard laminates, to which off-axis orientation is then applied, and to standard designs which possess *Extension-Shearing* without the requirement for off-axis alignment. Designs are matched for buckling strength with maximum *Extension-Shearing* coupling and a material strength assessment is then made.

2 BACKGROUND

The introduction of passive *Bending-Twisting* coupling at the wing-box level has been demonstrated [1] through *Extension-Shearing* coupling at the laminate level, i.e., the wing skins, for which there is a limited design space for *Extension-Shearing* coupling [7] with standard ply laminates (with 0°, ±45° and 90° ply orientations). By contrast, a substantial design space exists for laminates

with *Extension-Shearing* and *Bending-Twisting* coupling [8], yet care must be exercised, since the presence of *Bending-Twisting* coupling leads to a significant reduction in buckling strength [9].

Double angle-ply laminates have been shown to offer potential improvements in strength [10], together with ease of manufacturability [11], when compared to standard ply laminates. However, little consideration has been given to bending stiffness.

The normal practice of choosing the extensional stiffness first, typically by applying certain ply percentages, offers the possibility of shuffling the stacking sequence, within the constraints of the symmetric design rule for standard laminates, to optimise the buckling strength. However, this usually leads to the introduction of *Bending-Twisting* behaviour, which more often than not leads to a penalty in the buckling strength. The methodology adopted here traces a desired buckling strength to match a required material strength target.

3 METHODOLOGY

This article follows on from a recent study focusing on bending stiffness matching [12], and the development of a new database of double angle-ply laminate configurations containing specific mechanical coupling characteristics. The stiffness matching approach is used here to develop designs with bending isotropy, to which off-axis orientations can then be applied in order to introduce *Extension-Shearing* coupling for first ply failure assessment.

The development of a passive adaptive *Bending-Twisting* coupled wing requires E*xtension-Shearing* coupled laminate skins [2], which can be achieved in several ways. The following types of laminates are used for the design process:

1. off-axis alignment of otherwise balanced and symmetric laminates with standard ply orientations (0°, ±45° and 90°)
2. off-axis orientation of double angle-ply (±ϕ° and ±ψ°) laminates, with otherwise *Uncoupled* properties
3. *Extension-Shearing* coupled (only) laminates with standard ply orientations

A non-symmetric isotropic laminate configuration with standard ply orientations is also used as a datum to compare against the coupled designs:

$$[45/90/0/-45/0/-45/90/-45/45/0/45/90/45/90/-45/90/0/45/0/-45/0/-45/45/90]_T \quad (1)$$

The designs are fixed to 24 plies laminates, which represents the minimum ply number grouping for $\pi/4$ isotropy.

The balanced and symmetric design has the stacking sequence:

$$[-45/45/0_3/45/0/-45/0/90/0/90]_S \quad (2)$$

The stacking sequence is selected from the 24 plies laminate database, since it produces the highest Extension-Shearing coupling, measured as A_{16}/A_{11} = 21.9% at off-axis orientation, β = 37.3°. Note that the application of off-axis alignment also introduces non-zero lamination parameters ξ_3 and ξ_4., giving (ξ_1, ξ_2, ξ_3, ξ_4) = (0.09, -0.29, 0.32, 0.17). Beforehand the lamination parameter (ξ_1, ξ_2) = (0.33, 0.33). The lamination parameter and extensional stiffnesses, A_{ij}, are related through Eqn (9).

For the double angle-ply configuration designs, a new design methodology is adopted [12], which uses a technique to match the bending stiffness between standard ply laminates (with 0°, ±45° and 90° fibre directions) and double angle-ply laminates (with ±ϕ° and ±ψ° fibre directions). The conventional fibre directions, 0, 90 and ±45° now replaced with ±$\phi_{(\gamma)}$ and ±$\psi_{(1\ -\ \gamma)}$ pairs, where γ represents the proportion of ±ϕ, and (1 - γ) represents the proportion of ±ψ. For extension stiffness matching, these proportions correspond to the ±ϕ and ±ψ ply percentages. For bending stiffness matching, the proportions correspond to the relative contribution to bending stiffness of ±ϕ and ±ψ plies in the

laminate. The relative contribution to bending stiffness of the ±ϕ angle-ply sub-laminate in terms of lamination parameters is given by:

$$\zeta_{\pm\phi} = (\xi_9 - \beta)/(\alpha - \beta) \tag{3}$$

$$\begin{aligned} \alpha &= \cos 2\phi \\ \beta &= \cos 2\psi \end{aligned} \tag{4}$$

where, and β can be expressed in the form of a quadratic equation:

$$\beta = -(\xi_{10} + 1 - 2\alpha^2)/4(\alpha - \xi_9) \pm [((\xi_{10} + 1 - 2\alpha^2)/4(\alpha - \xi_9))^2 - (2\alpha^2\xi_9 - \alpha - \xi_{10}\alpha)/2(\alpha - \xi_9)]^{½} \tag{5}$$

which leads to a solution for angle ϕ from Eqn. 4 (solved iteratively), when Equations (3) and (5) are matched for the desired lamination parameters (ξ_9, ξ_{10}). Finally, a solution for angle ψ is obtained directly from Eqn. 4, once the iterative process has converged.

Stacking sequences, lamination parameters and angles ϕ and ψ from a previous study [12] are listed in Table 1. The angles were derived from Eqns (3) – (5) for (ξ_9, ξ_{10}) = (0, 0).

	Stacking sequence	ϕ,ψ	ξ_1,ξ_2
a	$[\psi/-\psi/-\phi/\phi/\phi/-\phi/\phi/-\phi/-\phi/\phi/-\psi/\psi/-\psi/\psi/\phi/-\phi/-\phi/\phi/-\phi/\phi/\phi/-\phi/\psi/-\psi]_T$	63.78,17.44	-0.13,-0.06
b	$[\psi/-\psi/\phi/-\phi/-\phi/\phi/-\phi/\phi/-\psi/\psi/\phi/-\phi/\phi/-\phi/-\psi/\psi/-\phi/\phi/-\phi/\phi/\phi/-\phi/\psi/-\psi]_T$	65.08,19.58	-0.17,-0.04
c	$[\psi/-\psi/-\phi/\phi/\phi/-\phi/-\psi/\psi/\phi/-\phi/-\phi/\phi/\phi/-\phi/-\phi/\phi/-\psi/\psi/-\phi/\phi/\phi/-\phi/\psi/-\psi]_T$	68.06,23.04	-0.25,0.01
d	$[\psi/-\psi/-\phi/\phi/-\psi/\psi/\phi/-\phi/\phi/-\phi/\phi/-\phi/-\phi/\phi/-\phi/\phi/-\phi/\phi/-\psi/\psi/\phi/-\phi/\psi/-\psi]_T$	74.28,27.06	-0.37,0.20
e	$[\psi/-\psi/\phi/-\phi/-\phi/\phi/\psi/-\psi/-\psi/\psi/-\psi/\psi/-\psi/\psi/-\psi/\psi/\psi/-\psi/-\phi/\phi/\phi/-\phi/\psi/-\psi]_T$	70.46,24.95	0.17,-0.05
f	$[\psi/-\psi/\phi/-\phi/\psi/-\psi/-\phi/\phi/-\psi/\psi/-\psi/\psi/-\psi/\psi/-\psi/\psi/-\phi/\phi/\psi/-\psi/\phi/-\phi/\psi/-\psi]_T$	78.64,28.59	0.05,-0.04

Table 1: Stacking sequences for fully uncoupled double angle-ply laminates with 24 layers. Angles (ϕ, ψ) produce bending isotropy.

The *Extension-Shearing* coupled laminate with standard ply orientations:

$$[45/90/0/-45/0/-45/90/-45/45/0/45/90/45/90/-45/90/0/45/0/-45/0/-45/45/90]_T \tag{6}$$

was derived using an algorithm developed previously [7]. The design has a maximum A_{16}/A_{11} of 16.7%, without off-axis alignment, and shares the same compression buckling strength as the isotropic plate, as can be readily confirmed from the closed form solution of Eqn (7), given that the design is fully uncoupled in bending, i.e., $D_{16} = D_{26} = 0$.

$$N_x = \pi^2 \left[D_{11} \left[\frac{m}{a} \right]^2 + 2\left(D_{12} + 2D_{66}\right)\frac{1}{b^2} + D_{22} \left[\frac{1}{b^4} \right] \left[\frac{a}{m} \right]^2 \right] \tag{7}$$

where *a* and *b* are the length and width of the laminate, *m* is the number of half-waves of the buckling mode along the plate length and D_{ij} are the elements of the bending stiffness matrix [**D**], which can be expressed in terms of lamination parameters by:

$$D_{11} = (U_1 + \xi_9 U_2 + \xi_{10} U_3) H^3/12 \quad D_{12} = (-\xi_{10} U_3 + U_4) H^3/12 \quad D_{16} = (\xi_{11} U_2/2 + \xi_{12} U_3) H^3/12$$
$$D_{22} = (U_1 - \xi_9 U_2 + \xi_{10} U_3) H^3/12 \quad D_{26} = (\xi_{11} U_2/2 - \xi_{12} U_3) \times H^3/12 \quad (8)$$
$$D_{66} = (-\xi_{10} U_3 + U_5) \times H^3/12$$

The elements of the extensional stiffness matrix [**A**], on which the material failure assessment is made, can also be expressed in terms of lamination parameters by:

$$A_{11} = (U_1 + \xi_1 U_2 + \xi_2 U_3) \times H \quad A_{12} = (-\xi_2 U_3 + U_4) \times H \quad A_{16} = (\xi_3 U_2/2 + \xi_4 U_3) \times H$$
$$A_{22} = (U_1 - \xi_1 U_2 + \xi_2 U_3) \times H \quad A_{26} = (\xi_3 U_2/2 - \xi_4 U_3) \times H \quad (9)$$
$$A_{66} = (-\xi_2 U_3 + U_5) \times H$$

where U_i is the invariants given by:

$$\begin{aligned} U_1 &= \left(3Q_{11} + 3Q_{22} + 2Q_{12} + 4Q_{66}\right)/8 \\ U_2 &= \left(Q_{11} - Q_{22}\right)/2 \\ U_3 &= \left(Q_{11} + Q_{22} - 2Q_{12} - 4Q_{66}\right)/8 \\ U_4 &= \left(Q_{11} + Q_{22} + 6Q_{12} - 4Q_{66}\right)/8 \\ U_5 &= \left(Q_{11} + Q_{22} - 2Q_{12} + 4Q_{66}\right)/8 \end{aligned} \quad (10)$$

The reduced stiffness are given by:

$$Q_{11} = E_1/1 - \nu_{12}\nu_{21},\ Q_{12} = \nu_{12}E_1/1 - \nu_{12}\nu_{21},\ Q_{22} = E_2/1 - \nu_{12}\nu_{21},\ Q_{66} = G_{12} \quad (11)$$

Noting that $E_1/\nu_{12} = E_2/\nu_{21}$.

The lamination parameter is given by:

$$\begin{aligned} \xi_1 &= \left\{n_{\pm}\cos(2\phi) + n_{\pm}\cos(2\psi)\right\}/n,\ \xi_2 = \left\{n_{\pm}\cos(4\phi) + n_{\pm}\cos(4\psi)\right\}/n \\ \xi_3 &= \left\{n_{\pm}\sin(2\phi) + n_{\pm}\sin(2\psi)\right\}/n,\ \xi_4 = \left\{n_{\pm}\sin(4\phi) + n_{\pm}\sin(4\psi)\right\}/n \\ \xi_9 &= \left\{\zeta_{\phi}\cos(2\phi) + \zeta_{\psi}\cos(2\psi)\right\}/\zeta,\ \xi_{10} = \left\{\zeta_{\phi}\cos(4\phi) + \zeta_{\psi}\cos(4\psi)\right\}/\zeta \\ \xi_{11} &= \left\{\zeta_{\phi}\sin(2\phi) + \zeta_{\psi}\sin(2\psi)\right\}/\zeta,\ \xi_{12} = \left\{\zeta_{\phi}\cos(2\phi) + \zeta_{\psi}\cos(2\psi)\right\}/\zeta \end{aligned} \quad (12)$$

where $\zeta = n^3$.

The Tsai-Wu failure criteria is used for the strength assessment and is defined by:

$$F_1\sigma_1 + F_2\sigma_2 + F_{11}\sigma_1^2 + F_{222}{}^2 + F_{66}\tau_{12}{}^2 - \left(F_{11}F_{22}\right)^{1/2}\sigma_1\sigma_2 = 1 \quad (13)$$

where

$$
\begin{aligned}
F_1 &= (1/\sigma_1^T + 1/\sigma_1^C) \\
F_2 &= (1/\sigma_2^T + 1/\sigma_2^C) \\
F_{11} &= -1/\sigma_1^T\sigma_1^C \\
F_{22} &= -1/\sigma_2^T\sigma_2^C \\
F_{66} &= (1/\tau_{12}^F)^2
\end{aligned}
\tag{14}
$$

Individual terms correspond to the strength constraint data listed in Table 2, for T300/5208 graphite/epoxy material adopted in this study.

E_1	181.0 GPa	σ_{1T}	1500
E_2	10.3 GPa	σ_{1C}	-1500
G_{12}	7.17 GPa	σ_{2T}	40
ν_{12}	0.28	σ_{2C}	-246
		τ_{12F}	68

Table 2: Engineering properties of T300/5208 graphite/epoxy.

The stiffness matching approach is now extended to simultaneously match first ply failure and buckling strength constraints for a chosen double angle-ply laminate with maximised *Extension-Shearing* coupling.

The results presented are based on compression buckling load, N_x, of a rectangular, simply supported plate with fixed aspect ratio, *a*/*b*, which for the uncoupled designs adopted here allows the use of the closed form buckling solution of Eqn (7). The procedure involves simultaneously matching the load for both buckling and first ply failure, from which physical plate dimensions *a* and *b*. can be determined.

4 RESULTS

The six double angle-ply designs share two unique sets of extension stiffness properties, hence there are only two points on the lamination parameter design spaces for extensional stiffness. Designs ***a***, ***b***, ***c*** and ***d*** share one of the unique points and ***e*** and ***f*** share the other. The bending stiffnesses are however all different.

The double angle ply designs are far from the in-plane lamination parameters (ξ_1, ξ_2) for typical aircraft components: Spar (0, -0.6), Skin (0.32, 0.12) and Stiffener (0.5, 0.4), which correspond, respectively, to the following ply percentages for 0°, ±45° and 90° ply orientations: Spar (10/80/10), Skin (44/44/12) and Stiffener (60/30/10). However, if the angles are switched, such that the outer plies become ϕ rather than ψ the design space becomes a mirror image and the solutions are found to be in close proximity to a typical Skin component, for which buckling strength and material strength constraints coincide at some point along a wing structure.

The results are therefore reported with the ϕ and ψ in the double angle-ply laminate designs stacking sequences switched. However, for bending isotropy to be maintained in the designs reported in Table 1, the values of ϕ and ψ must be modified as follows:

$$
\begin{aligned}
\phi_{switched} &= 90° - \psi \\
\psi_{switched} &= 90° - \phi
\end{aligned}
\tag{15}
$$

Figure 1(a) and (b) represent the lamination parameter design spaces for extensional and bending stiffness double angle-ply laminate design ***d,*** with line indicating constant buckling load of a square plate superimposed on the design spaces. The overall compression for aspect ratio (*a*/*b* =) 1 and 1.5

are superimposed onto the bending stiffness design spaces of laminate design ***d*** on Fig. 1(c) and (d), respectively.

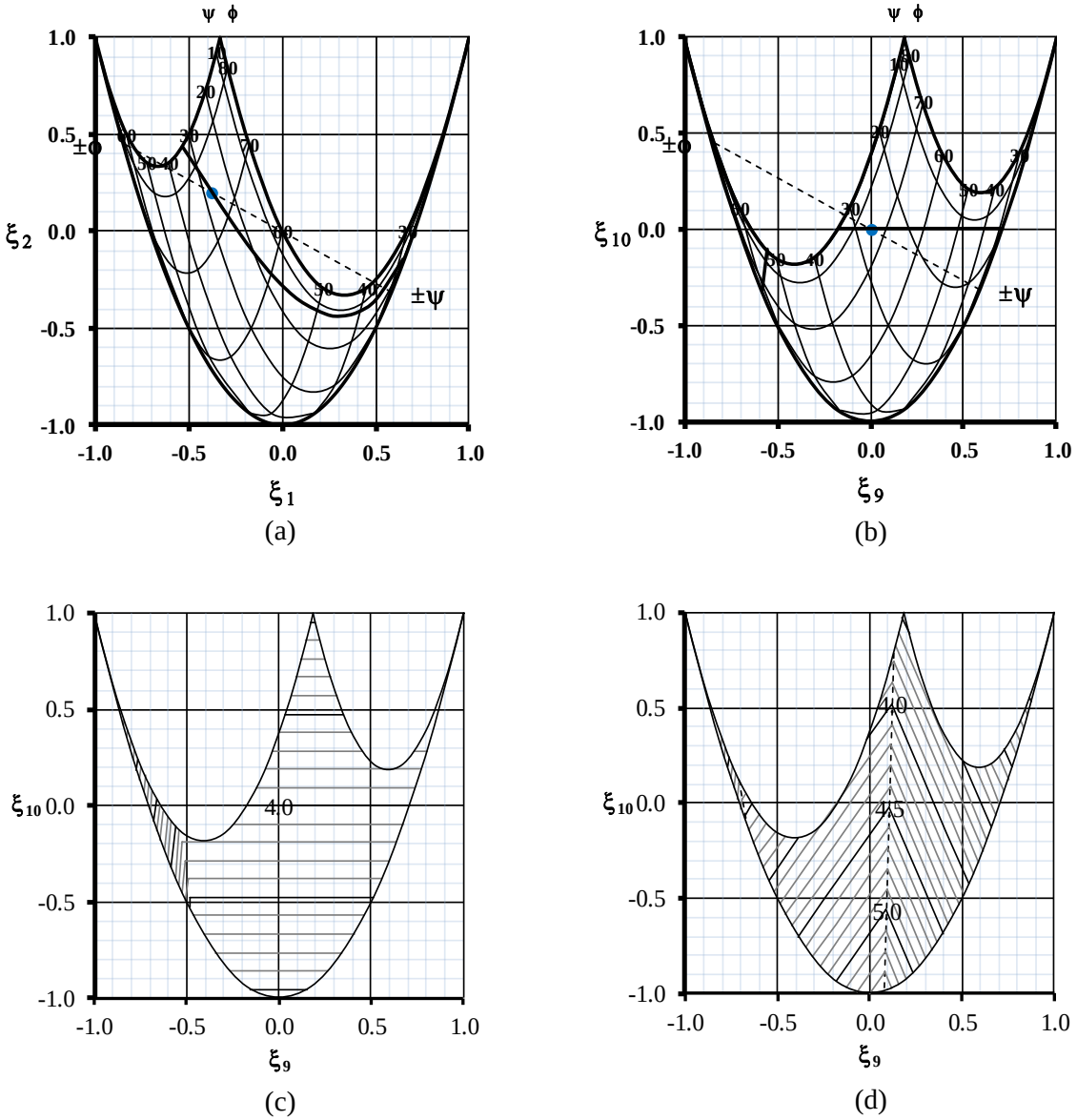

Figure 1: Lamination parameter design spaces for laminate ***d*** from Table 1 corresponding to (a) extension stiffness and; (b) bending stiffness, with the lines of constant compression buckling factor k_x = 4.0. Compression buckling contour maps for aspect ratio (c) a/b = 1.0 and; (d) a/b = 1.5.

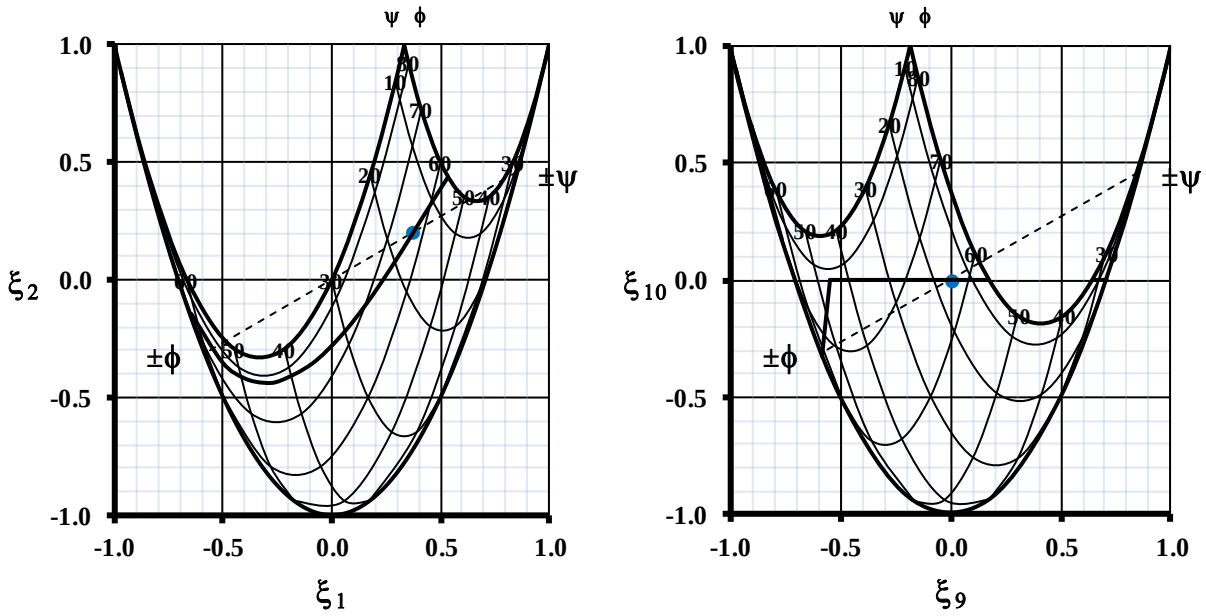

(a) (b)

Figure 2: Feasible design space for (a) extension stiffness and; (b) bending stiffness with lines representing constant compression buckling factor, $k_x = 4.0$.

Figure 2 represents the extension and bending stiffness design spaces with a superimposed compression buckling line of $k_x = 4.0$ for the angles switched double angle design laminate ***d***. Figure 1(a), (b) and Fig. 2 illustrate that it is possible to design double angle-ply laminates with the classical buckling factor of 4.0.

The compressive load (N_x), given by Eqn (7), corresponding to the minimum first ply failure after off-axis orientation, is used to normalise all the polar plots that follow. The double angle-ply laminate ***d*** was found to have the lowest first ply failure load (605.3 N/mm).

Figure 3(a) and (b) represent bubble plots of the first ply failure strength of double angle ply laminate ***d*** at 10° increments across the design space. The line $k_x = 4.0$ is superimposed on both Fig. 3(a) and (b). Figure 3(c) and (d) show bubble plots of standard ply angles with the 10% rule applied and onto which the double angle ply laminate designs ***a***, ***b***, ***c*** and ***d*** are superimposed for comparisons. The Tsai-Wu failure criterion is used to assess uniaxial compression strength, which is proportional to bubble area, normalized with respect to the 0° ply laminate, with lamination parameter (ξ_1, ξ_2) = (1, 1), which has the highest failure strength. Only the results for double angle-ply laminates ***a*** to ***d*** are given on Fig. 3(a) and (b). The location of typical aircraft wing skin designs is also plotted on the lamination design space of Fig. 3(b), (c) and (d) for comparison with the double angle-ply laminates.

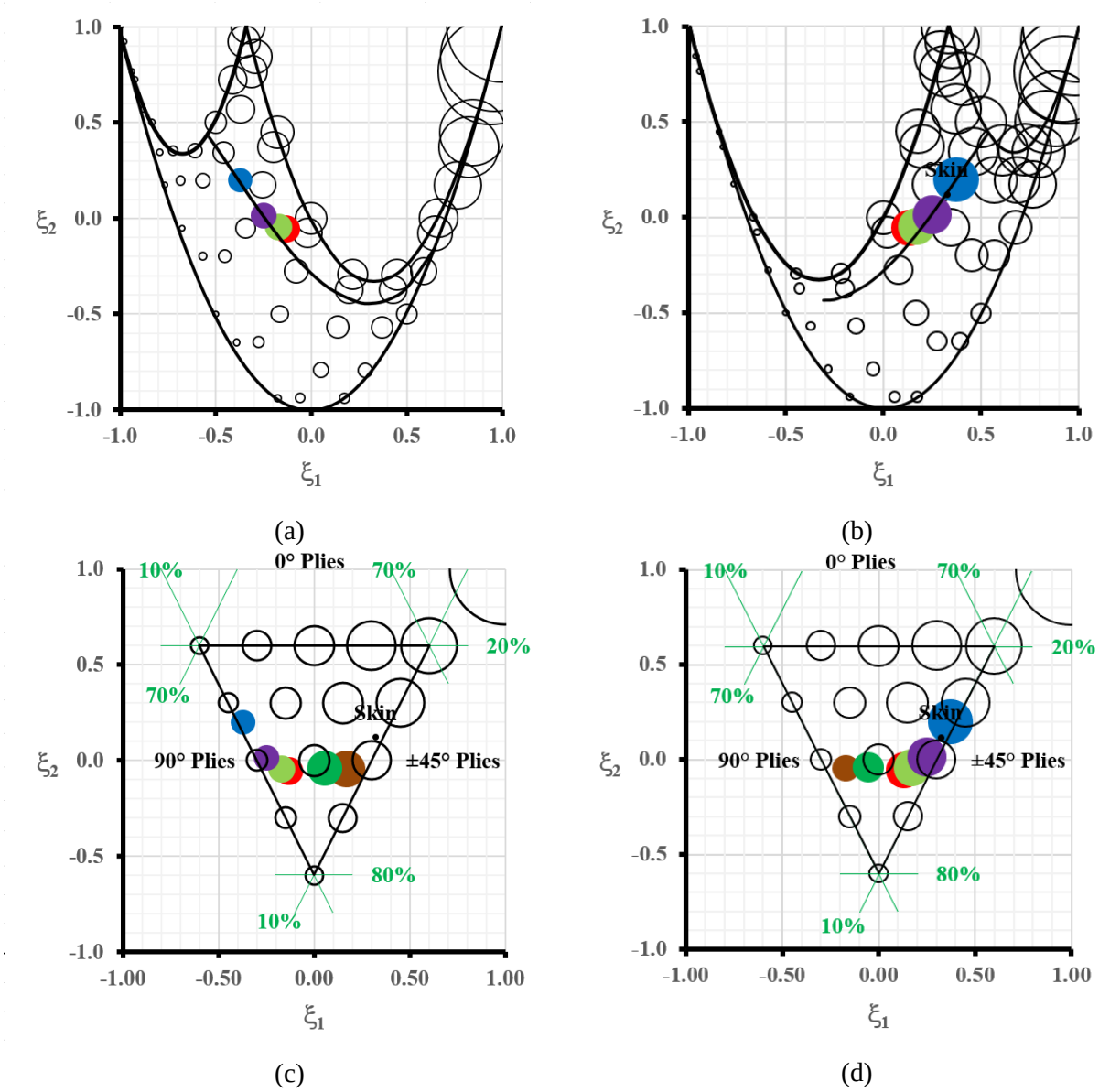

Figure 3: Strength comparisons for fully uncoupled Standard laminates (satisfying 10% rule) and Double angle-ply laminates for stacking sequence ***a***, ***b***, ***c*** and ***d*** with angles: (a) as listed in Table 1; (b) switched. Standard laminates are superimposed on designs ***a*** to ***f*** with angles as: (c) listed in Table 1 and; (d) switched. Strength values are indicated by bubble area, normalized against maximum (100%) strength for 0° ply laminate shown at $(\xi_1, \xi_2) = (1, 1)$.

Figure 3(a) and (b) illustrate the potential to optimize laminates for strength without degrading the buckling strength by choosing designs along the buckling line indicated bold on Fig. 2. This implies that the strength of composite laminates can be improved without the reduction of buckling load. The equivalent line of constant buckling factor $k_x = 4.0$ is plotted on Fig. 3 (a) and (b), revealing that the line on Fig. 3(b) is very close to the typical location of aircraft wing skin configuration. It can be seen that the design ***e*** and ***f***, with $(\xi_1, \xi_2) = (0.17, -0.05)$ and $(0.05, -0.04)$ respectively, have higher failure strength than designs ***a***, ***b***, ***c*** and ***d***, but with angles switched using Eqn. (15), design ***d*** has the highest strength compared to the other designs.

Strength values are indicated by bubble area, normalized against maximum (100%) strength for a 0° ply laminate shown at $(\xi_1, \xi_2) = (1, 1)$. This was chosen to reflect the test procedure for determining laminate strength data. Laminate ***d*** has a normalised strength of 6.2%, in Fig. 3(a), and with angles switched has a normalised strength of 10.3%, in Fig. 3(b).

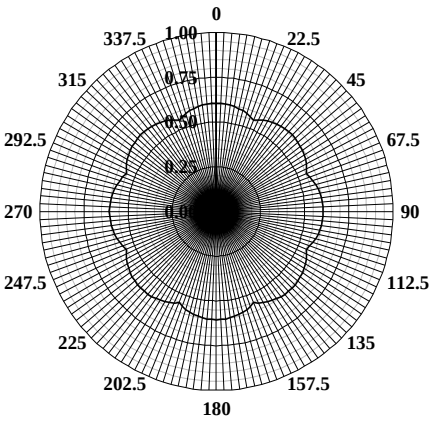

(a) Isotropic

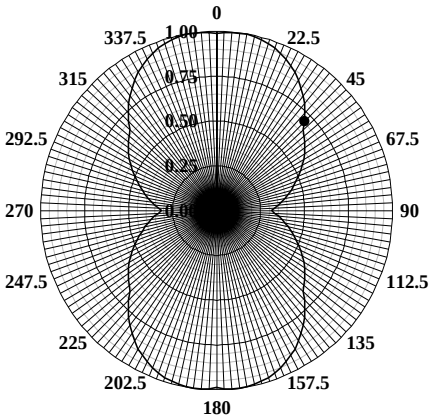

(b) Max A_{16}/A_{11} = -22.1% at β = 46.1°.

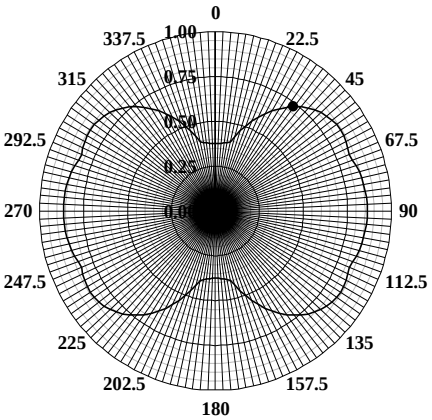

(c) Max A_{16}/A_{11} = 21.9% at β = 37.3°.

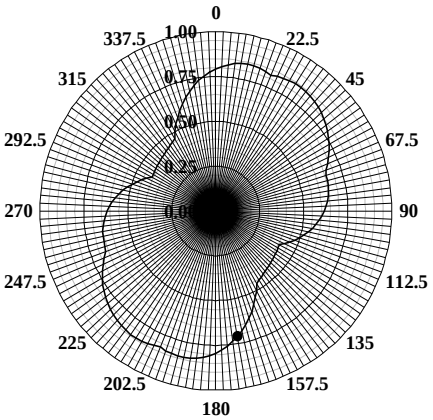

(d) Max A_{16}/A_{11} = 16.3% at β = 0°.
A_{16}/A_{11} = 18.0% at β = 170.1°

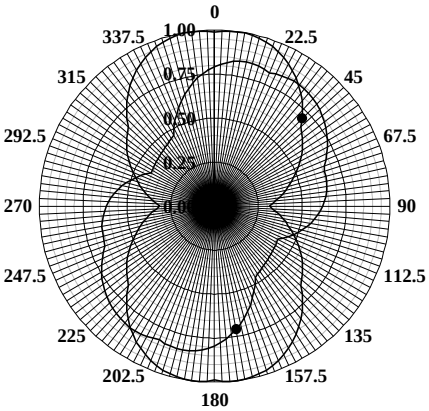

(e) Laminate ***d*** and *E-S* coupled outer envelopes.

Figure 4: Strength comparisons for off-axis orientation β between a full envelope of 24 ply: (a) Isotropic laminate; (b) Double angle-ply laminate design ***d***; (c) Balanced and symmetric; (d) *Extension-Shearing* coupled (only) design and; (e) Superimposed laminate ***d*** and Extension-Shearing coupled design, all subject to equal compressive force resultant (N_x).

Figure 4 represents polar plots of first ply failure with applied off-axis orientation, including double angle-ply laminate ***d***, balanced and symmetric, isotropic and *Extension-Shearing* coupled only laminates. All the designs are normalized against double angle-ply laminate ***d*** which has the lowest first ply failure load. The point on each figure denotes the value of β giving maximum A_{16}/A_{11}.

Here only laminate ***d*** is presented as it has the highest maximum A_{16}/A_{11} among all the double angle-ply designs. The angles switched laminates gives the same maximum A_{16}/A_{11} as their non-switched angles counter laminates. Normalised against the first ply failure load for laminate ***d*** (100% at β = ±7.1°), the balanced and symmetric design is at 37.5% of its material strength constraint and the *Extension-Shearing* coupled only laminate is at 79.3% (at β = 0°). However, at off-axis alignment, corresponding to maximum A_{16}/A_{11}, laminate ***d*** and the balanced and symmetric designs are at 68.9% (at β = 46.1°) and 73.1% (at β = 37.3°) of their material strength constraint, respectively.

Normalising against the first ply failure load for a 0° ply laminate, the Isotropic laminate has 8.5% of the first ply failure strength and the *Extension-Shearing* coupled only laminate has 5.5% (at β = 0°). For off-axis alignment, corresponding to maximum A_{16}/A_{11}, laminate ***d*** and the balanced and symmetric designs are at 6.2% (at β = 46.1°) and 5.8% (at β = 37.3°) of the first ply failure strength, respectively.

Table 3 presents the required width, *b*, for coincident buckling and first ply failure under compression load of the double angle-ply laminate designs for aspect ratio *a*/*b* = 1.0, 1.5, 2.0 and 2.5. The dimensions are typical of the width between stiffeners in a stiffened panel wing skin. Table 4 shows the width to total thickness (*H*) ratio, *b*/*H*, of the optimal designs in Table 3.

	Laminate design					
a/*b*	***a***	***b***	***c***	***d***	***e***	***f***
1, 2	107.7	110.7	116.5	124.5	92.0	98.6
1.5	112.1	115.3	121.4	129.6	95.8	102.7
2.5	109.4	112.6	118.5	126.5	93.5	100.2

Table 3: Plate width, *b*, corresponding to 24 ply double angle-ply design with coincident buckling and first ply failure.

	Laminate design					
a/*b*	***a***	***b***	***c***	***d***	***e***	***f***
1, 2	32.1	33.0	34.8	37.1	27.4	29.4
1.5	33.4	34.4	36.2	38.7	28.6	30.6
2.5	32.6	33.6	35.3	37.7	27.9	29.9

Table 4: Width to thickness ratio, *b*/*H*, corresponding to optimal 24 ply double angle-ply designs in Table 3.

5 CONCLUSIONS

This article has explored the design spaces of double angle-ply designs, which match the equivalent ply percentages of typical aircraft skin designs. The effect of off-axis alignment on the first ply failure performance of laminates is also demonstrated. Moreover, this article has attempted to size the double angle-ply laminates through buckling and strength constraints.

Polar plot of first ply failure have demonstrated that double angle-ply designs offer comparable strength to standard laminates when off-axis orientation is applied to maximise anisotropy or *Extension-Shear* coupling.

The design approach used to achieve optimised material strength and anisotropy has been shown to be possible without degrading buckling performance of various standard and double angle-ply designs.

REFERENCES

[1] C. V. Jutte and B. K. Stanford, Aeroelastic tailoring of transport aircraft wings: state-of-the-art and potential enabling technologies, *NASA/TM-2014-218525*, 2014.

[2] C. B. York, Y. B. Murta and S. F. M Almeida, A Passive-adaptive Wing for Drag Reduction, *31st Congress of the International Council of the Aeronautical Sciences*, Belo Horizonte, Brazil, 2018.

[3] Z. Gürdal, R. T. Haftka and P. Hajela, *Design and optimization of laminated composite materials*, John Wiley & Sons, New York, 1999.

[4] C. B. York, Buckling analysis and minimum-mass design procedures for composite wing-box structures. *Journal of Aircraft*, 43(2), 2006, pp. 528-536.

[5] H. A Deveci, L. Aydin and H. S. Artem, Buckling optimization of composite laminates using a hybrid algorithm under Puck failure criterion constraint, *Journal of Reinforced Plastics and Composites*, **35**(16), 2016, pp. 1233 – 1247.

[6] R. H. Lopez, M. A. Luersenb and E. S. Cursi, Optimization of laminated composites considering different failure criteria, *Composites: Part B*, **40**, 2009, pp. 731 – 740.

[7] C. B. York "On extension-shearing coupled laminates". *Composite Structures*, Vol. 120, pp. 472-482, 2015.

[8] C. B. York and S. F. M. Almeida, On extension-shearing bending-twisting coupled laminates". *Composite Structures*, **164**, 2017, pp. 10-22.

[9] C. B. York. On bending-twisting coupled laminates, *Composite Structures*, **160**, 2017, pp. 887-900.

[10] S. Tsai, Keynote: design of composite laminates, *21st International Conference on Composite Materials*, Xi'an, China, 2017.

[11] M. W. D. Nielsen, K. J. Johnson, A. T. Rhead and R. Butler, Laminate design for optimised in-plane performance and ease of manufacture, *Composite structures*, **177**, 2018, pp. 119-128.

[12] C. B. York, New insights into stiffness matching between standard and double angle-ply laminates, *11th Asian-Australian Conference on Composite Materials*, Cairns, Australia, 2018.